scientific reports

Check for updates

OPEN

Subcytotoxic transepidermal delivery using low intensity cold atmospheric plasma

Ga Ram Ahn[1,2,3,9], Hyung-Joon Park[4,9], Yu Jin Kim[3,9], Min Gyo Song[5], Hye Sung Han[3,6], Woo Geon Lee[3], Hyuck Ki Hong[7], Kwang Ho Yoo[3,6], Joon Seok[2,3,10]✉, Kyu Back Lee[5,8,10]✉ & Beom Joon Kim[2,3,10]✉

Cold atmospheric plasma (CAP) has been utilized in various medical devices using its oxidative nature. Recent studies have provided evidence that CAP can facilitate the delivery of large, hydrophilic molecules through the epidermis to the dermis. On the other hand, a new approach called low-intensity CAP (LICAP) has been developed, allowing the plasma level to be controlled within a subtoxic range, thereby demonstrating various biological benefits without tissue damage. However, the ability of LICAP to enhance transepidermal delivery in sub-cytotoxic conditions has not been fully investigated. This study aims to determine the sub-cytotoxic range of exposure time for LICAP and, within the range, to investigate the effects of LICAP treatment on transepidermal drug delivery (TED) and mechanisms using human keratinocytes and a mouse model. For the in vitro studies, LICAP treatment was evaluated in human keratinocyte (HaCaT) cells by assessing reactive species production, DNA damage, and cytotoxicity profiles. Within the determined safety range, mechanistic analyses were conducted to examine LICAP-enhanced delivery pathways. mRNA expression and protein levels of tight and adherens junction genes were quantified, and changes in ultramicroscopic morphology of HaCaT monolayers were investigated. Intracellular delivery of fluorescein isothiocyanate (FITC)-dextran was also assessed. For the in vivo studies, E-cadherin expression and the transepidermal delivery (TED) of human epidermal growth factor (hEGF) were analyzed in LICAP-treated mouse dorsal skin. The upper safety range of LICAP exposure time, reducing cell viability by 70% (IC70 or LD30), was estimated at 34.3 s. Within the safety range, LICAP treatment downregulated multiple tight and adherens junction genes in HaCaT cells. Consistent with the in vitro results, the epidermal E-cadherin expression was reduced, and human epidermal growth factor (hEGF) was infiltrated in the dermis of the LICAP-treated mouse skin. Intercellular clefts were detected in the HaCaT cell monolayer immediately following LICAP treatment and intracellular delivery of FITC-dextran was confirmed after LICAP exposure. This study demonstrated that LICAP treatment enhances transepidermal permeation of hEGF, apparently via both paracellular and transcellular routes. Under our study conditions, LICAP treatment seems to be a novel approach to facilitate TED with low safety concerns in vitro. Further translational studies are needed for clinical evaluation.

Keywords Cold atmospheric plasma, Cytotoxicity, Hormesis, Low intensity, LICAP, Plasma jet, Transepidermal delivery, Drug delivery

[1]Department of Dermatology, Cutaneous Biology Research Center, Massachusetts General Hospital, Harvard Medical School, Boston, MA, USA. [2]Department of Dermatology, Chung-Ang University Hospital, 102, Heukseok-ro, Dongjak-gu, Seoul, Republic of Korea. [3]College of Medicine, Chung-Ang University, Seoul, Korea. [4]Department of Interdisciplinary Bio/Micro System Technology, College of Engineering, Korea University, Seoul, Republic of Korea. [5]Department of Biomedical Engineering, College of Health Science, Korea University, Seoul, Republic of Korea. [6]Department of Dermatology, Chung-Ang University Gwangmyeong Hospital, Gwangmyeong-si, Gyeonggi-do, Republic of Korea. [7]Human IT Convergence System R&D Division, Korea Electronics Technology Institute, Seongnam-si, Gyeonggi-do, Republic of Korea. [8]BK21 Four R&E Center for Precision Public Health, Korea University, Seoul, Republic of Korea. [9]These author contributed equally: Ga Ram Ahn, Hyung-Joon Park, and Yu Jin Kim [10]These author corresponding authorship shared: Joon Seok, Kyu Back Lee and Beom Joon Kim ✉email: seokjoon923@gmail.com; kblee@korea.ac.kr; beomjoon74@gmail.com

Abbreviations

CAM	Cell adhesion molecule
CAP	Cold atmospheric plasma
DAPI	4′,6-Diamidino-2-phenylindole
DCF	Dichlorofluorescein
DMEM	Dulbecco's modified eagle's medium
ELISA	Enzyme-linked immunosorbent assay
FBS	Fetal bovine serum
FITC	Fluorescein isothiocyanate
hEGF	Human epidermal growth factor
HRP	Horseradish peroxidase
IC50	50% inhibitory concentration
IC70	70% inhibitory concentration
IHC	Immunohistochemistry
LD30	30% lethal dose
LICAP	Low-intensity cold atmospheric plasma
MTT	3-(4,5-Dimethylthiazol-2-yl)-2,5-diphenyltetrazolium bromide
NIH	National institutes of health
PBS	Phosphate-buffered saline
qPCR	Quantitative polymerase chain reaction
RS	Reactive species
SC	Stratum corneum
SEM	Scanning electron microscopy
TED	Transepidermal delivery

Topical agents including drugs and cosmetics are the mainstay of the therapeutic arsenal for dermatologists[1]. However, the low efficiency of epidermal permeability often impedes their effectiveness. Various energy-based devices (EBDs) capable of improving transepidermal delivery (TED) have been proposed and utilized in combination with topical agents to overcome this obstacle[2–5].

Cold atmospheric plasma (CAP) is a low-temperature (< 40 °C) physical plasma generated under atmospheric pressure using an electric field. CAP delivers reactive species to tissues and is used medically for controlled cell or tissue destruction, such as in cancer treatment, sterilization, and skin resurfacing[6–8]. Interestingly, recent studies have demonstrated low-intensity exposure of CAP—low enough to maintain cellular viability—can enhance the transdermal penetration of substances with large molecular sizes or hydrophilic properties without peeling off the skin barrier[9–15]. This novel application of plasma, recently named as low-intensity cold atmospheric plasma (LICAP) treatment, has shown promising results in non-ablative wrinkle reduction and skin whitening as well[16,17].

On the other hand, recent interest has surged in trans-epidermal delivery (TED), a method for delivering bio-stimulating molecules to the dermis, using CAP[10–13,15,18,19]. This approach is distinct from the conventional trans-"dermal" drug delivery which primarily focuses on transporting large molecules, such as vaccines or insulin, across the skin into the systemic circulation[20–22]. For the paracellular route, some reports suggest that CAP-induced TED enhancement is related to the temporal suppression of E-cadherin, one of the proteins that composes cell adhesion molecules (CAMs)[18,19]. However, the effect on other proteins composing the CAM complex that seals the intercellular space to inhibit percutaneous, i.e., tight and adherens junctions has not been investigated[24]. In addition to decreased expression, some data indicate that CAP can promote immediate intercellular detachment that may facilitate intercellular passage[25–28]. For the transcellular route, on the other hand, there is substantial evidence that CAP can enhance membrane permeability and facilitate the delivery of large hydrophilic molecules through the plasma membrane[12,29–51].

In addition, for the safe and successful therapeutic application of CAP, the safety limit dose in terms of cytotoxicity must be determined because the highly oxidative plasma produces reactive species (RS) in the target, and excessive exposure might cause cell death[6]. However, data for estimating the in vitro cytotoxicity profiles of CAP devices that are developed to enhance TED are scarce, and previous investigations have mostly focused on the effect or potential mechanisms[18,19].

Therefore, the aims of our study are as follows: (1) to establish the safety range of a novel LICAP device at the cell level, (2) to confirm the effect of LICAP treatment within the safe range to enhance the transepidermal penetration of a large protein complex (i.e., human epidermal growth factor, approximately 6000 Da) and (3) to explore the possible biological mechanisms of the enhanced passage of large hydrophilic molecules through the epidermal barrier to explore potential routes for TED.

Materials and methods

LICAP device

An FDA-approved plasma jet device (U.S. Food and Drug Administration regulation number: 21 CFR 878.4400) was used in this study (PlazMagik®, AGNES Medical Co., Gyeonggi-do, Republic of Korea) (Fig. 1a). N50 (99.999%) helium gas was used as the plasma vehicle gas with a gas flow rate of 0.12 L/min (0.009 MPa). The plasma was generated under a radiofrequency of 12 kHz and a power of 35.2 W. The plasma jet stream was exposed at each target (in vitro: solution media surface, in vivo: mouse dorsum) at a target surface-to-nozzle tip height of 8 mm (Fig. 1b–d). The device and its sterile disposable tips were manufactured in a current Good Manufacturing Practice (cGMP) facility. The sterile disposable tips were replaced for each experiment, and the device was subjected to UV sterilization before and after each test.

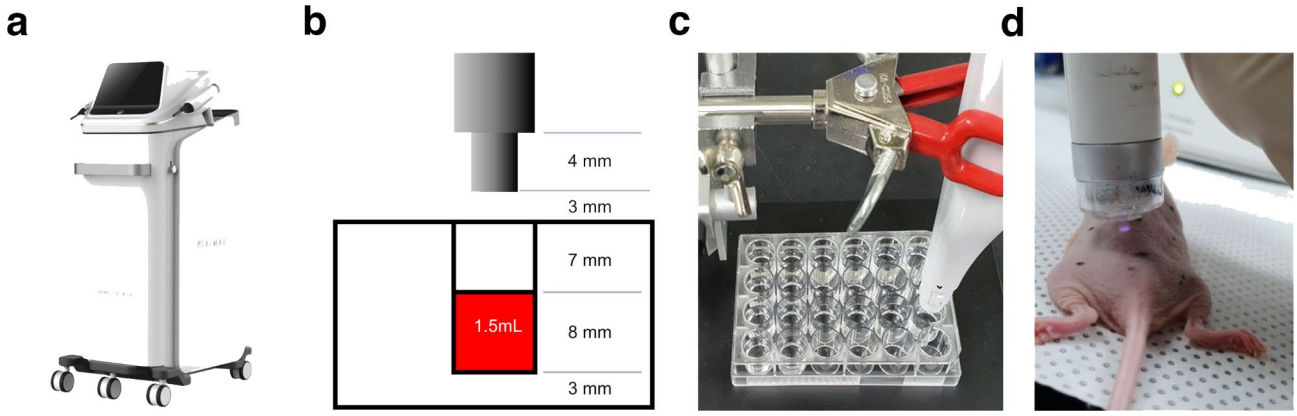

Fig. 1. Images of test device (**a**) and setting of in vitro (**b**,**c**) and in vivo (**d**) plasma exposure.

RS production assay

The production of RS was evaluated using the standard protocol of the OxiSelect® in vitro ROS/RNS assay kit (STA-347, Cell Biolabs, Co., CA, USA) to determine its correlation with plasma exposure time. The wells of a 24-well plate were each filled with 1.5 ml of phosphate-buffered saline (PBS) (SH30256, Hyclone®, MA, USA). PBS was selected as a target solution since it has physiological osmolality and buffered acidity (pH 7.7). The helium plasma from the LICAP device was exposed for 5, 10, 15, 20, 25, and 30 s 8 mm above the surface of the PBS solution. After plasma exposure, each sample received 50 µL of catalyst and was incubated for 5 min. Each well was then filled with 100 µL of dichlorofluorescein (DCF) solution. The plate was then read at 480/530 nm wavelengths using a plate reader (VICTORX3®, Perkin Elmer, MA, USA) to determine the level of RS production.

In vitro

HaCaT cell preparation for thein vitro assay

For the in vitro experiments, human keratinocyte cells (HaCaT cells) were purchased from ATGC, Co. (Seoul). The cells were grown in Dulbecco's modified Eagle's medium (DMEM) (11965092, Gibco-BRL, NY, USA) containing 10% fetal bovine serum (FBS) (10082147, Thermo Fisher Scientific, MA, USA), 100 U/mL penicillin G, and 100 g/mL streptomycin (15140122, Thermo Fisher Scientific, MA, USA) in a humidified atmosphere containing 5% carbon dioxide.

Cell viability test

To determine the viability of cells following LICAP treatment, a 3-(4,5-dimethylthiazol-2-yl)-2,5-diphenyl-2 H-tetrazolium bromide (MTT) (ab211091, Abcam, Cambridge, England) assay was used[52]. A 24-well plate was seeded with 7.2×10^5 cells. Plasma was applied at 8 mm above the media surface for durations ranging from 0 to 600 s. After plasma treatment, the cells were incubated. Following a 24-h incubation period, the media was removed from each well. Subsequently, 250 µL of MTT reagent and 250 µL of media were added to each well and incubated for 1 h. After the incubation, the MTT reagent was removed, and 750 µL of DMSO was added to each well. The plate was then placed on a plate shaker for 15 min to ensure thorough mixing. Absorbance was measured at 540 nm. Cell viability was calculated as a percentage of untreated controls. The exposure time needed to reduce cell viability by 70% (IC_{70}) was determined as upper safety range of LICAP[53].

DNA damage assay

A 24-well plate was seeded with 7.2×10^5 cells. Plasma was applied at a predetermined intensity at a height of 8 mm above the media surface in the 24-well plate for 0, 5, 10, 15, 20, 25, 30, 60, and 120 s, followed by incubation for 24 h. G-DEXTM IIe genomic DNA extraction kit (17231, iNtRON Biotechnology, Gyeonggi-do, Korea) was used to extract cell DNA (iNtRON Biotechnology). DNA was denatured at 95 °C for 10 min and cooled on ice for 10 min. To determine the DNA damage of cells following LICAP treatment, the 8-hydroxy-2-deoxyguanosine enzyme-linked immunosorbent assay (ELISA) kit measured RS-induced DNA damage (ab211154, Abcam, Cambridge, England). The plate was read at 450 nm and the sample absorbance was compared with the standard curve to determine DNA damage.

Quantitative polymerase chain reaction

HaCaT cells were seeded in 6-well plates and treated with LICAP for 0, 5, 10, 15, 20, 25, and 30 s. The cells were then collected at 0, 3, 6, and 24 h after treatment. For the qPCR analysis, total RNA was extracted from HaCaT cells using TRIzol reagent (1596028, Invitrogen, CA, USA) according to the manufacturer's instructions. First-strand cDNA synthesis from the total RNA template was performed with PrimeScriptTM RT master mix (RR036A, Takara, Tokyo, Japan). The resulting cDNA was subjected to real-time PCR using qPCR 2x PreMIX SYBR (RT500S, Enzynomics, Seoul, Korea) and a CFX-96 thermocycler (CFX-96®, Bio-Rad, CA, USA). The PCR conditions used to amplify all genes were as follows: 10 min at 95 °C and 40 cycles of 95 °C for 10 s and 60 °C for 15 s, and 70 °C for 30 s. Expression data were calculated from the cycle threshold (Ct) value using the ΔCt

method of quantification. Glyceraldehyde 3-phosphate dehydrogenase (GAPDH) was used for normalization. The sequence of each primer is listed in the supplementary data (Fig.S1).

Western blot

HaCaT cells were seeded in 6-well plates and treated with LICAP for 0, 5, 10, 15, 20, 25, and 30 s. The cells were then collected at 0, 3, 6, and 24 h after treatment. Protein lysates were prepared using RIPA buffer (89900, Thermo Fisher Scientific, MA, USA). The protein lysates were resolved on 10% SDS-PAGE gels and electrotransferred to a nitrocellulose membrane (15279794, Cytiva, Amersham, USA). After blocking with 5% skim milk in Tris-buffered saline containing 0.5% Tween-20 (TBST), membranes were probed with anti-claudin1 (1:2500; ab24584; Abcam, Cambridge, UK), anti-Occludin (1:2500; ab68; Abcam), anti-E-cadherin (1:2500; ab85679; Abcam), and anti-β-actin (1:1000; sc-47778; Santa Cruz Biotechnology) antibodies at 4 °C overnight. After washing, membranes were incubated with horseradish peroxidase (HRP)-conjugated anti-mouse (PI-2000-1, Vector Laboratories Inc., CA, USA) or anti-rabbit (PI-9500-1, Vector Laboratories Inc., CA, USA) secondary antibodies. Immunoreactive signals were detected using an Amersham ECL kit (12316992, GE Healthcare, IL, USA), according to the manufacturer's instructions. The results were visualized with the ChemiDoc™ MP Imaging System (12003154, Bio-Rad Laboratories, Inc., CA, USA). The resulting blots were analyzed using Image J software (National Institutes of Health, Bethesda, MD, USA).

Intracellular delivery in LICAP-treated HaCaT cells

The intracellular delivery of Fluorescein isothiocyanate (FITC)-dextran was measured in HaCaT cells treated with LICAP for 30 s to examine the possibility of enhancement of transepidermal drug penetration by LICAP in human skin. FITC-dextran with a molecular weight of 3000–5000 Da was purchased from Sigma-Aldrich, Co. (68059, MA, USA). HaCaT cells grown in Dulbecco's modified Eagle's medium (DMEM) (11965092, Gibco-BRL, NY, USA) supplemented with 10% FBS were treated with LICAP for 30 s, followed by a 24-h incubation with FITC-dextran. Using an optical microscope, bright-field and fluorescence images were captured and are displayed in the manuscript as merged images.

SEM of the LICAP-treated HaCaT cell monolayer

Scanning electron microscopy (SEM) (JSM-6701 F®, JEOL, Japan) was used to detect the immediate morphological changes in the intercellular region between human keratinocytes. To obtain the HaCaT cell monolayer, the cells were seeded in a six-well plate containing DMEM with 10% FBS and incubated at 37 °C in an incubator containing 5% CO_2. The medium was replaced every two days until the cell density reached 80%. LICAP was applied to the monolayer for 30 s, and the samples were fixed for 24 h with 2.5% glutaraldehyde in 0.1 M phosphate buffer (pH 7.4). After being washed with 0.1 M phosphate buffer, the samples were postfixed in 1% OsO_4 in 0.1 M phosphate buffer for 1 h before being dehydrated through a series of ethanol concentrations. The dried samples were coated with gold using a sputtering technique and analyzed using a scanning electron microscope. The images were captured at ×1000 and ×2000 magnification to detect the immediate morphological changes in the intercellular region between human keratinocytes and are displayed in the manuscript.

In vivo

Animal model for thein vivo assay

A total of forty six-week-old female hairless mice (HRM1; Saeron Bio Inc., Korea) were used in the study. The mice were fed antibiotic-free solid food and water ad libitum and acclimatized for one week in a controlled environment with a temperature of 23.2 °C, humidity of 55.0%, and a 12-h light-dark cycle. All animal experiments were approved by Chung-Ang University's Institutional Animal Care and Use Committee (IACUC) and conducted in compliance with National Institutes of Health (NIH) regulations for laboratory animal care and the ARRIVE guidelines 2.0 (https://arriveguidelines.org).

For each in vivo test, the mice were divided into groups with $n = 5$: five groups for the immunohistochemistry (IHC) study (untreated, 0 h, 3 h, 6 h, and 24 h) and three groups for the hEGF study (untreated, immediately after treatment, and 24 h after treatment). The dorsal area of each mouse was divided into four 1 cm × 1 cm sections, with each section irradiated with plasma for 30 s generated at 12 kHz and 35.2 W. The treatment spots were sufficiently spaced apart to prevent inter-spot effects, with the device's handpiece physically enclosing each treatment spot to minimize the diffusion of reactive oxygen species (ROS) and ensure independent tissue-plasma interactions. The average value from the four treatment areas of each mouse was used to represent the data for that mouse. Tissues were collected after CO2 euthanasia at different time points according to each study design.

IHC assay for epidermal E-cadherin

For the IHC assay, each skin sample of the hairless mouse was 10% formalin-fixed, paraffin-embedded, and sectioned to a thickness of 5 µm. Using a 10 mM citrate buffer, the sections were deparaffinized, rehydrated, and subjected to antigen retrieval. Endogenous peroxidase activity was inhibited with 3% hydrogen peroxide, and the sections were incubated with a 1:200 dilution of an anti-E-cadherin primary antibody (14472. Cell signaling technology, MA, USA). The sections were then incubated with a secondary antibody conjugated with HRP, and the signal was detected using a substrate containing 3,3′-diaminobenzidine. The stained slides were counterstained with hematoxylin, photographed using a slide scanner (Pannoramic MIDI®, 3DHISTECH Ltd, Budapest, Hungary), and observed using CaseViewer® software (3DHISTECH Ltd) to measure the E-cadherin-stained area in the epidermal region of interest. The quantitative analysis was based on the color density values measured in ten independent square regions of interest with a side length of 50 µm at the papillary dermis level, avoiding epidermal involutions, skin appendages, and cysts. This was done using independent scanned immunofluorescence images with dimensions of 1210 × 910 µm (1920 × 1440 pixels, x10 magnification).

Transepidermal penetration in mouse skin

An anti-His-tag antibody was used in an immunofluorescence assay to detect hEGF skin penetration (Santa Cruz Biotechnology, Co., Dallas, TX, USA). 1 cc (5 mg/dL) of hEGF was topically applied on mouse dorsum. The isolated tissues were fixed with 4% paraformaldehyde overnight and embedded in paraffin. In accordance with the manufacturer's instructions, an anti-His-tag antibody was used to stain the 5-μm-thick section. The nuclei were counterstained with 4',6-diamidino-2-phenylindole (DAPI, #AR-6501-01, Immuno Bioscience Corp., Washington, USA) following secondary staining with an Alexa 488-conjugated goat anti-rabbit IgG antibody (Thermo Fisher Scientific, Co.). A Carl Zeiss LSM 780® confocal laser microscope (Carl Zeiss, Baden-Württemberg, Germany) was used to image fluorescent staining of exogenous EGF. The same strategy as in the IHC study was used to calculate the relative absorption rate of exogenous EGF by comparing the fluorescence intensity of the untreated control.

Statistical analysis

All numerical data were collected in triplicate, and the results are expressed as the mean ± standard deviation (SD). One-way analysis of variance (ANOVA) and Tukey's post hoc analysis were used to determine statistically significant differences between groups. The statistical significance of p-values is denoted by an asterisk (*) and a double asterisk (**) when the value was less than 0.05 and 0.01, respectively.

Results

Measurement of the cytotoxic profile of LICAP

Cell viability, RS production, and DNA damage were evaluated to confirm the safety margins of LICAP at the human keratinocyte level (Fig. 2).

The MTT assay was performed to measure the cytotoxicity of LICAP by exposure time (Fig. 2a). The graph of cell viability showed a sigmoidal decrease and showed a good fit with the following four-parameter logistic (4PL) curve:

$$y = \frac{5.414 - 101.9}{1 + \left(\frac{x}{52.18}\right)^{-1.679}} + 101.9 \ \left(R^2 = 0.9970\right).$$

The $IC_{50,}$ the representative value used to describe cytotoxicity, was 57.12 s. The IC_{70} (=LD_{30}), which is the minimal dose that can be considered to have cytotoxic effect, was 34.28 s[53].

The production of RS was gradually increased with increasing exposure time to the helium plasma jet from the LICAP device within the subcytotoxic range (Fig. 2b). The linearity showed a good fit with a simple linear regression model as follows:

$$y = 6.618 \times 10^{-4}x + 5.988 \times 10^{-4} \ (R^2 = 0.7204)$$

.

The concentration of 8-OHdG, a biomarker of oxidative DNA damage was increased as the LICAP exposure increased (Fig. 2c). The increment curve also showed a good fit with the following 4PL curve model:

$$y = \frac{1.762 - 2.512}{1 + \left(\frac{x}{43.77}\right)^{-2.421}} + 2.512 \ \left(R^2 = 0.7461\right).$$

Effect on the expression of cell adhesion molecules

Within the cytotoxically safe range, the mRNA expression of tight and adherens junction protein genes (i.e., claudin1, occludin, and E-cadherin) showed initial suppression, marked at 3 h post-treatment, followed by recovery within 24 h (Fig. 3a–e). The results of the western blot analysis were consistent with the qPCR data (Fig. 3f–k).

The in vitro data that showed temporal suppression and recovery of junctional proteins also appeared in the in vivo condition (Fig. 4). The epidermal E-cadherin expression in LICAP-treated mouse skin appeared to be reduced at 0 and 3 h after LICAP treatment and then recovered at 6 and 24 h (Fig. 4a–f). The decrement was significant at 0 h (-50.3 ± 11.7%, $p = 0.0004$) and 3 h (-64.6 ± 10.9%, $p < 0.0001$), while there was no significant reduction in the 6- and 24-h post-treatment groups ($p = 0.0631$ and 0.3754, respectively) (Fig. 4f).

Effect of LICAP treatment on transepidermal penetration

In the mouse model, the plasma exposure induced marked infiltration of hEGF in the dermis (Fig. 5a–j). The efficacy of TED was quantified using morphometrical analysis based on the fluorescence intensity of dermal hEGF (Fig. 5j). The skin samples obtained 0 and 24 h after LICAP treatment and topical hEGF application showed significantly ($p < 0.01$, both) increased dermal absorption of hEGF (50.0 ± 3.06% and 58.9 ± 3.56%, respectively).

SEM of the LICAP-treated HaCaT cell monolayer

Based on the in vivo data demonstrating the immediate dermal absorption of hEGF, we hypothesized that the unlatching of intercellular junction may occur immediately after exposure to LICAP. SEM was used to capture and visualize the morphological changes in the LICAP-treated HaCaT cell monolayer (Fig. 6). The treated

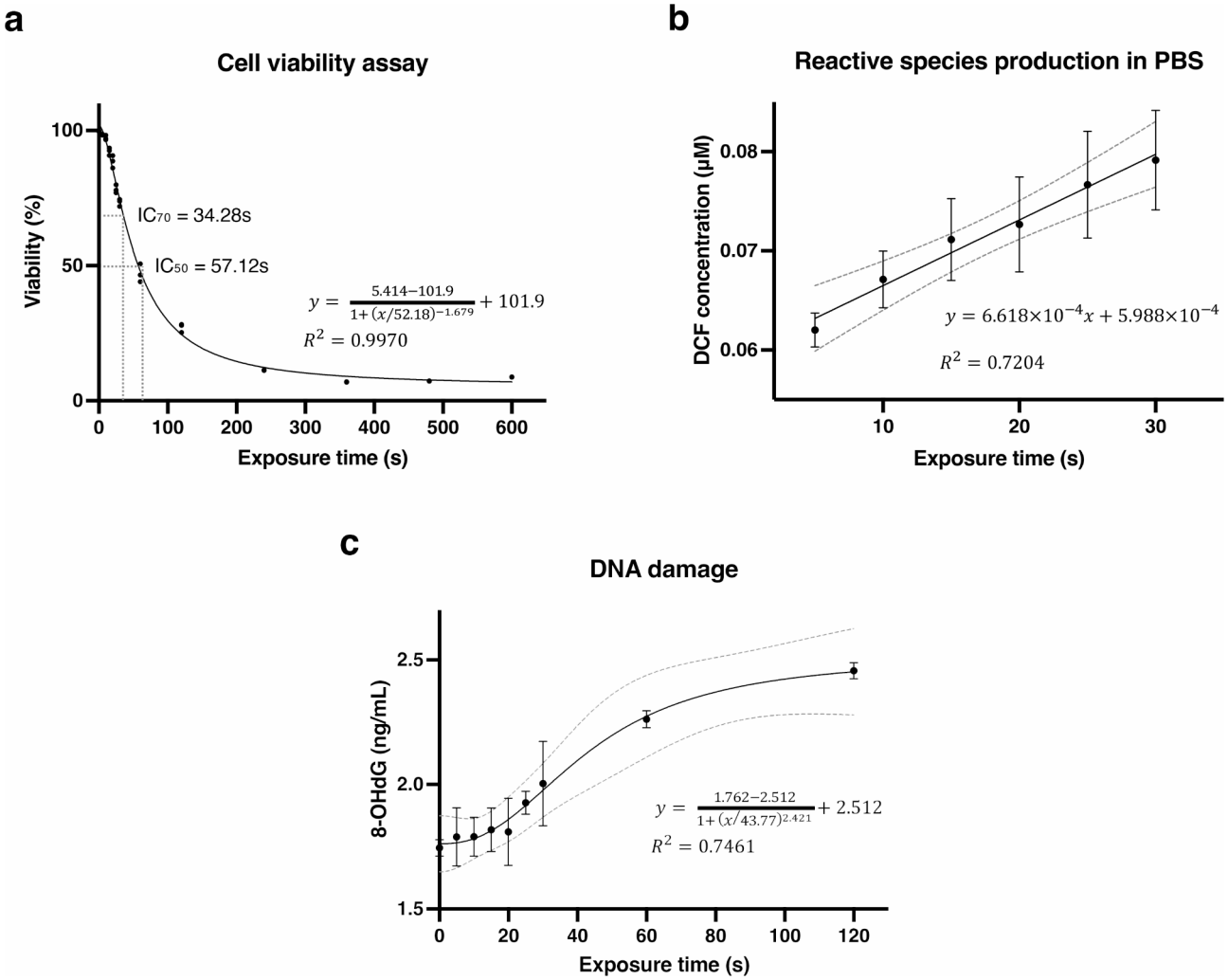

Fig. 2. Measurement data for cell viability, reactive species (RS) production, and DNA damage. In cell viability assay (**a**), The IC_{50} and IC_{70} values were 57.12 s and 34.28 s, respectively. The findings showed a good fit with a 4PL curve model ($R^2 = 0.7462$) The production of RS (**b**) increased linearly with an increasing exposure duration ($R^2 = 0.7244$). DNA damage (**c**) increased gradually with exposure time. The gray dashed lines represent the error ranges corresponding with a confidence interval of 95%.

samples were analyzed immediately following LICAP treatment for 30 s. In contrast to the untreated control samples (Fig. 6a), plasma-treated samples (Fig. 6b) exhibited intercellular clefts in numerous view fields.

Intracellular delivery in LICAP-treated HaCaT cells

After 24 h of incubation with dextran measuring 3000–5000 Da after LICAP treatment, FITC-dextran-laden keratinocytes were detected by bright-field (Fig. 6c,f) and fluorescence (Fig. 6d,g) microscope, whereas no FITC-dextran-containing cells were found in the untreated control group.

Discussion

This study aimed to investigate the potential of low-intensity cold atmospheric plasma (LICAP) in enhancing transepidermal permeability while maintaining cell viability. Our results demonstrate that LICAP treatment effectively increases the penetration of large, hydrophilic molecules (i.e., hEGF) through the epidermal barrier within the subcytotoxic range of LICAP exposure. Mechanistically, our data suggest that this enhanced delivery is related to increased permeability through both paracellular and transcellular pathways facilitated by LICAP exposure.

Cold atmospheric plasma (CAP) delivers oxidative species and was initially used for medical applications such as treating precancerous lesions, disinfection, and tissue welding[6]. When CAP was first introduced as a new anti-aging modality, dermatologists, who had been familiar with laser resurfacing since the late 1990s[54,55], initially applied CAP in a similar destructive manner for skin resurfacing[7,8]. However, the extensive downtime occasionally associated with skin resurfacing has led to a decline in its use in dermatology.

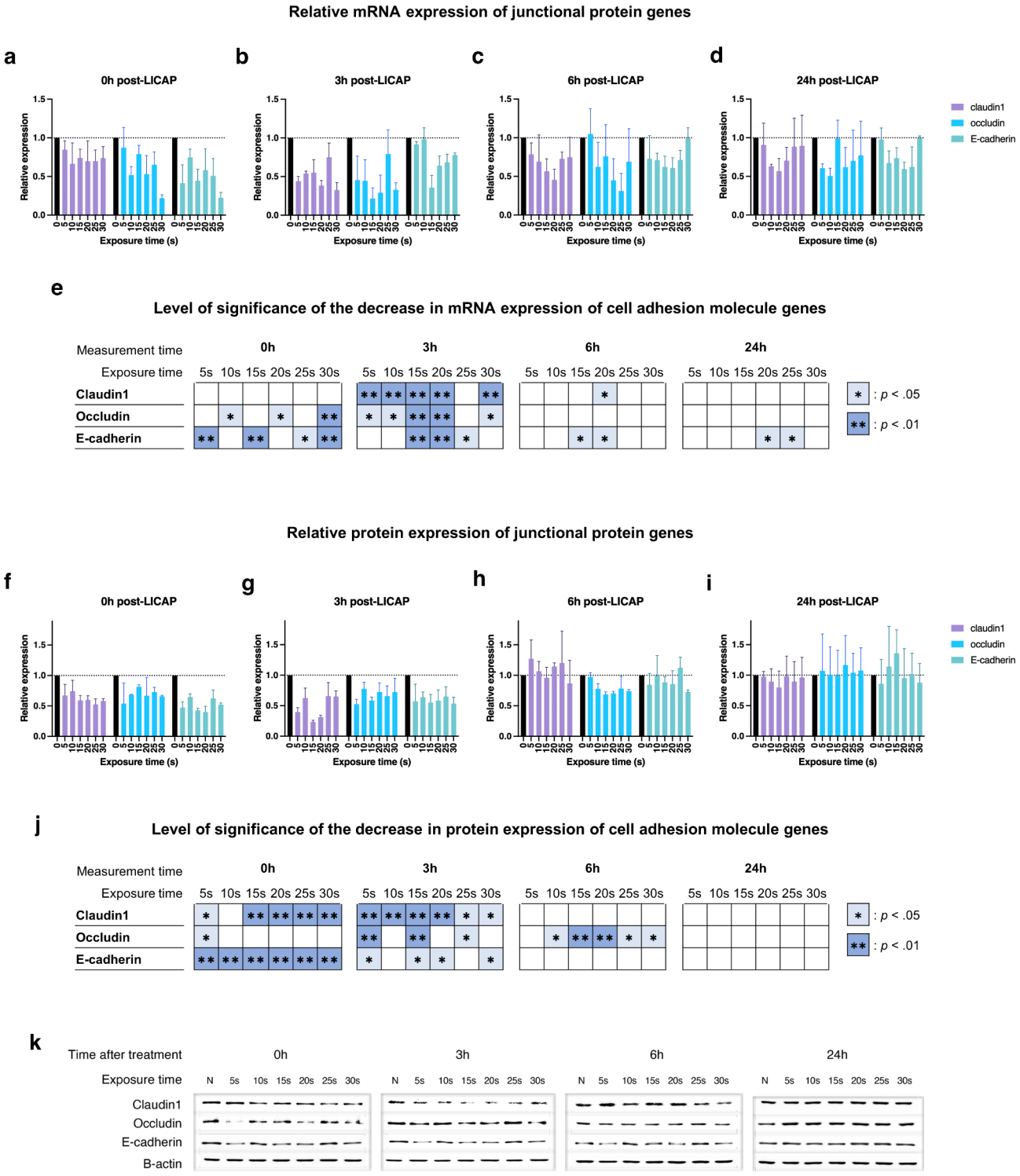

Fig. 3. Change in the mRNA expression of genes encoding cell adhesion molecules in HaCaT cells treated with plasma. The quantitative polymerase chain reaction results (**a**–**d**) were ordered by gene, plasma exposure time, and time after treatment. The level of comparative significance between the baseline and each timeline was arrayed in table (**e**). The data from western blot analysis of cell adhesion molecules in HaCaT cells treated with plasma are shown in (**f**–**k**). The quantitative data (**f**–**i**were arranged according to protein, plasma exposure time, and time after treatment. The level of comparative significance between the baseline and each timeline was presented in table (**j**). Following exposure to LICAP for a duration within the safe range (~ 30 s), the mRNA and protein levels of cell adhesion molecules were suppressed, marked at 3 h post-treatment, and eventually recovered.

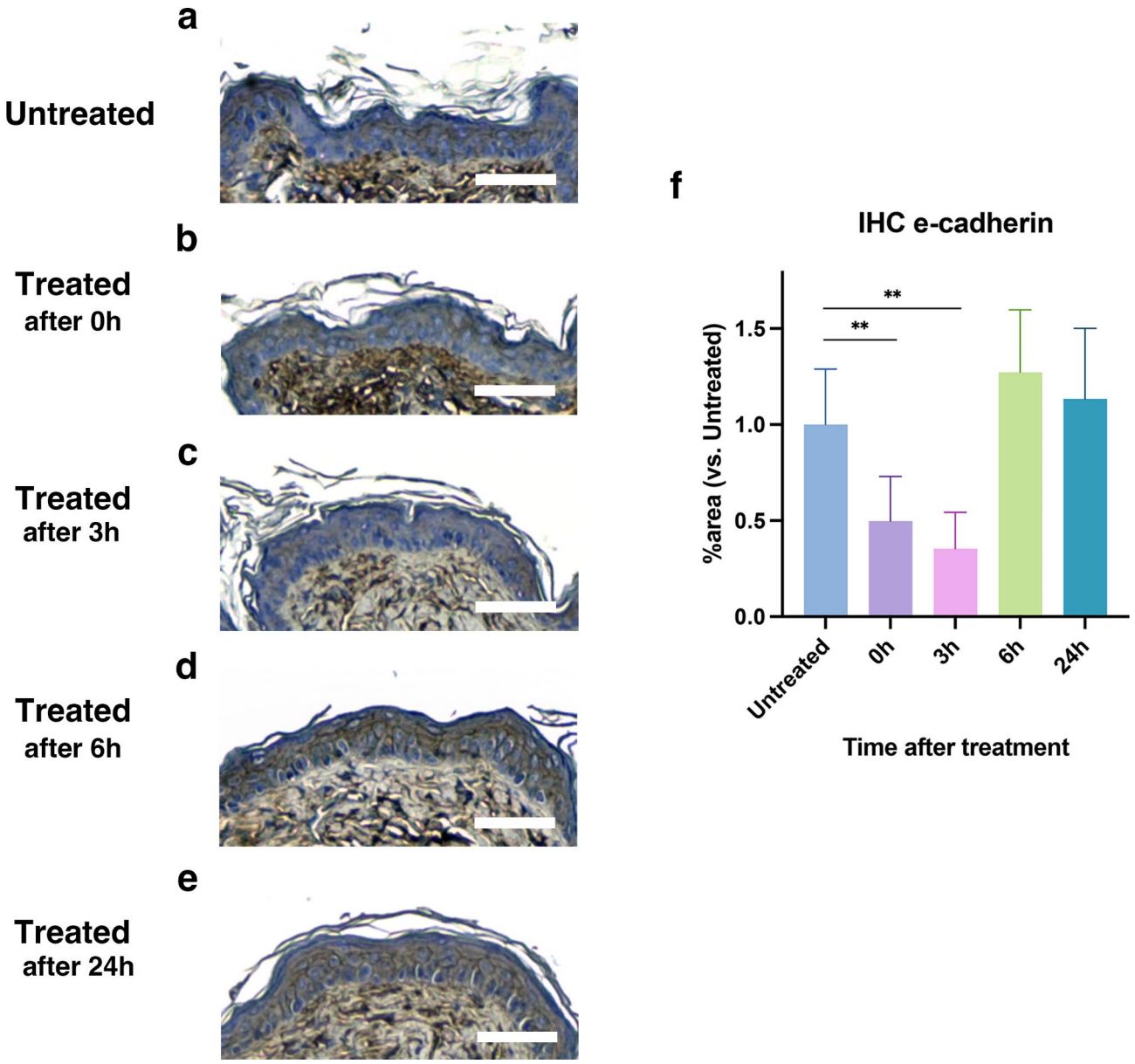

Fig. 4. Results of the IHC analysis of E-cadherin expression in the epidermis of LICAP-treated mouse skin. The expression of E-cadherin appeared to be decreased until 3 h after LICAP treatment (**b**,**c**) and then recovered 6 h after treatment (**d**) compared with the untreated control (**a**). The proportion of immunohistologically stained regions decreased significantly at 0 h (−50.3%) and 3 h (−64.6%) after LICAP therapy, while there was no significant reduction in the 6- and 24-h groups (**f**). Scale bar = 150 μm. The levels of statistical significance are indicated by * for $p < 0.05$ and ** for $p < 0.01$..

On the other hand, it has been recently shown that a low range of CAP exposure can activate endogenous antioxidant and anti-aging processes via the Nrf2 pathway, suggesting a possibility for non-destructive cell-preserving applications of CAP[56]. These anti-aging effects of non-destructive CAP have been observed in in vivo studies[16,17]. Additionally, the potential of CAP to facilitate epidermal penetration of large hydrophilic molecules has been suggested[15,18,19], leading to the present study exploring the use of non-destructive low-intensity CAP (LICAP) as a modality for TED. Please refer to Table 1 which compares conventional CAP and the novel concept of LICAP device[57].

Establishing the subcytotoxic range of LICAP verified its cell-preserving profile and provided a quantitative definition previously suggested in our studies: *"a physical plasma device that is designed to tune its plasma effluent intensity to a low range to enhance tissue (or cell) regeneration without damaging its viability"*[16,17].

In the quantitative view, the guidelines by the International Organization for Standardization (ISO) define the cytotoxic exposure dose range for medical devices as the range that causes a reduction in cell viability by 30% or more in the MTT assay[53]. In our results, the IC_{70} (= LD_{30}) value was estimated to be up to approximately

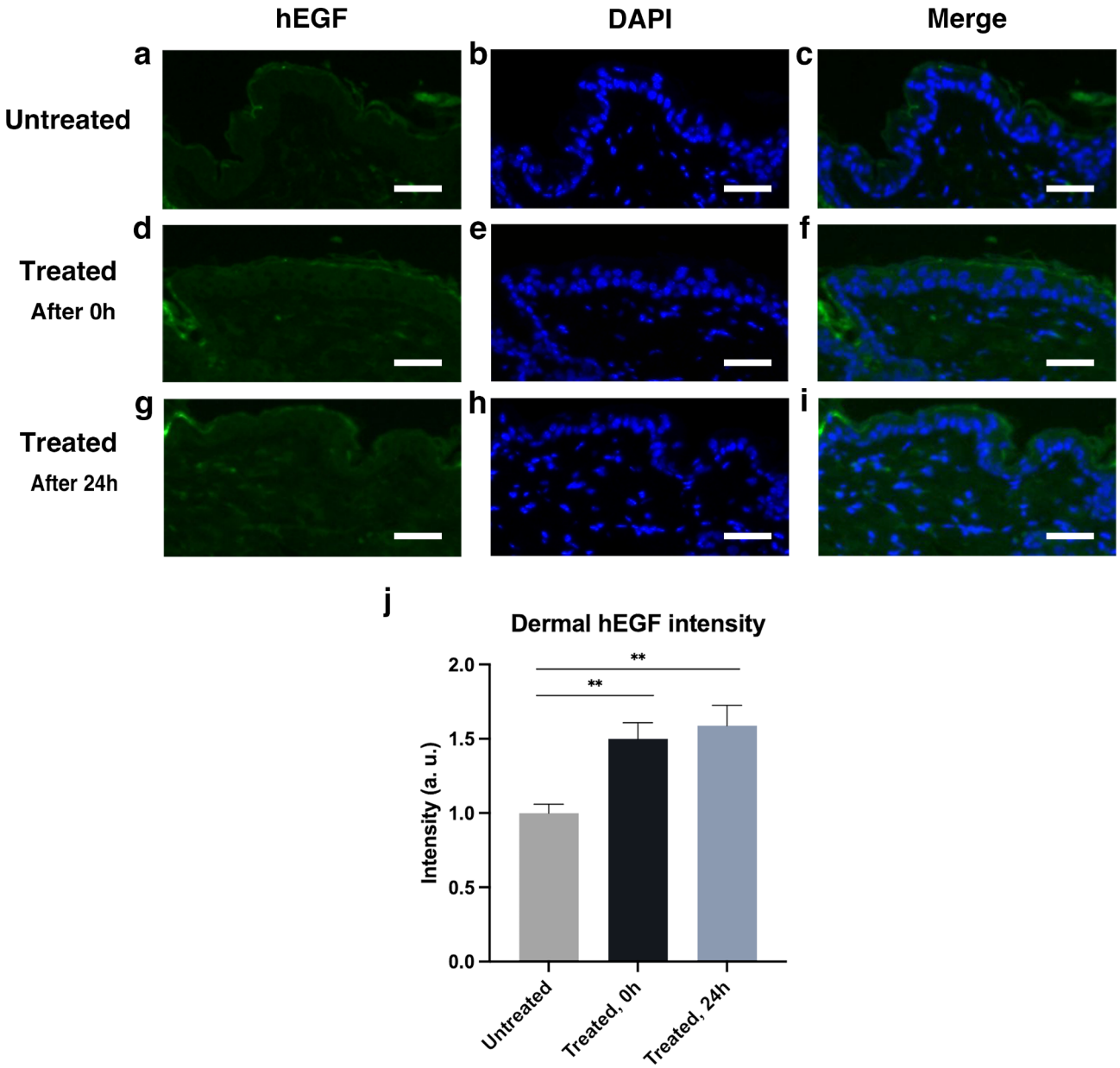

Fig. 5. Transepidermal diffusion of hEGF in plasma-treated skin. Compared with untreated skin (**a**–**c**), plasma-treated skin exhibited marked infiltration of hEGF in dermis (**d**–**i**). The fluorescence intensity from dermal hEGF was assessed via morphometrical analysis (j), which detected significant dermal absorption of hEGF in LICAP-treated skin; the fluorescence intensity of dermal hEGF was increased by 50.0% in the LICAP-treated skin immediately following the application and the dermal infiltration sustained for 24 h after treatment (58.9%) ($p < 0.01$, both). Scale bar = 150 μm. The levels of statistical significance are indicated by asterisks (* for $p < 0.05$ and ** for $p < 0.01$)..

30 s (34.3 s according to regression analysis). Therefore, all subsequent experiments were performed with plasma exposure within the subcytotoxic range of 30 s.

The hEGF immunofluorescence study demonstrated that the LICAP treatment used in this study is effective on TED aligned with previous studies in which the same molecule was used[18,19]. The first step for TED is to penetrate the stratum corneum (SC), a critical skin barrier. Since 2011, there has been abundant evidence suggesting that cold atmospheric plasma can facilitate the passage of drugs through the SC[9,10,12,13]. This facilitation can be explained by that cold atmospheric plasma creates pores in the SC, which is composed of tightly packed dead keratinocytes and an interspersed lipid layer[45,47,59,60]. After passing through the stratum corneum (SC), molecules only need to cross the epidermis layer to reach the dermis. There are two pathways for passing through the epidermis: the paracellular route, which involves movement between cells, and the transcellular route, which involves direct passage through the cells[61].

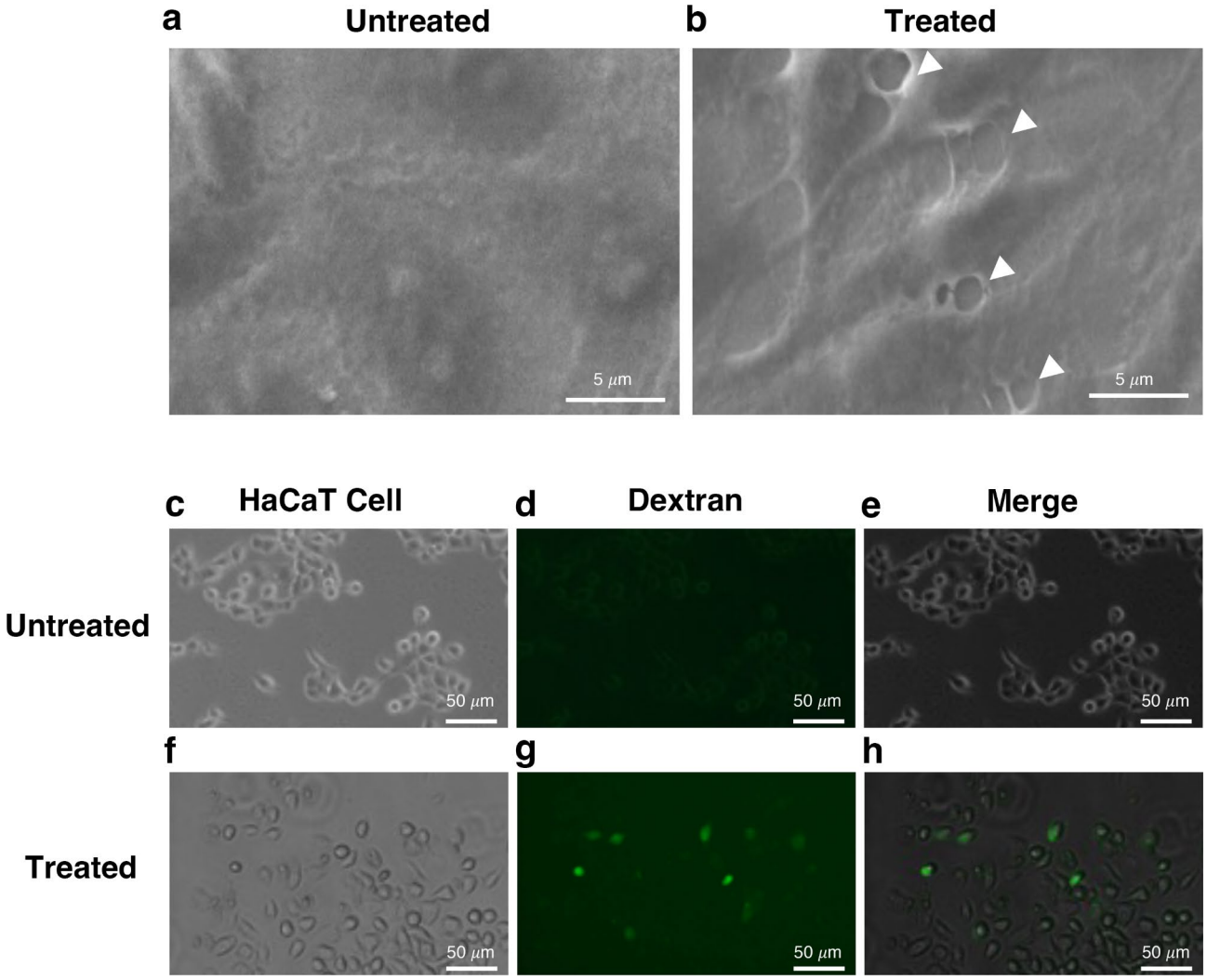

Fig. 6. Evidence of immediate intercellular cleft formation and intracellular delivery of hydrophilic, large molecule in LICAP-treated HaCaT cells. Compared to untreated HaCaT monolayer (**a**), LICAP-treated specimens (**b**) frequently exhibited intercellular clefts (white arrowheads) in numerous fields. The samples were examined immediately after the LICAP treatment for 30 s. Representative Bright-field (**c**,**f**), fluorescence (**d**,**g**), and merged (**e**,**h**) images caught intracellular delivery of fluorescein isothiocyanate-dextran (3000–5000 Da) in the plasma-treated group. Note the scale bar for the magnification.

Features	Conventional CAP[7,8]	LICAP
Plasma generation	Non-thermal (electric)	Non-thermal (electric)
Plasma intensity	High	Low
ROS/RNS level	High	Low and transient
Therapeutic window	Narrow	Wide
Cytotoxicity in clinical setting	Cytotoxic	Cell-preserving
Treatment mechanism	Controlled tissue damage and following recovery	Hormesis by intrinsic antioxidant pathway
Applications	Skin resurfacing[7,8], subdermal tightening[73,74]	Photoaging treatment[16,17,52], transepidermal drug delivery

Table 1. Comparison between the conventional cold atmospheric plasma (CAP) and low-intensity CAP (LICAP) for aesthetic application on skin surfaces.

The mRNA expression data indicates that TED enhancement is linked to transient suppression of junctional proteins. Our findings expand the explanation of Choi et al.[19] and Lee et al.[18], who demonstrated a temporal decrease in E-cadherin, which is a representative protein in intercellular adherens junction, expression and increment of TED of hEGF following CAP application on mouse skin. Besides the adherens junction, our data

revealed that LICAP treatment can also suppress the expression of tight junction proteins (i.e., claudin-1 and occludin). These proteins also play a crucial role as gatekeepers in TED[62]. This enhances the recently growing conjecture that the transient opening of the paracellular pathway may serve as a possible mechanism for LICAP-induced TED[15,17–19].

However, changes in gene expression was insufficient to explain the immediate TED effect when considering that dermal diffusion was also observed immediately after (0 h) the LICAP treatment. As a result, the next step was to investigate other candidates for TED routes that can be modulated immediately by CAP: The immediate partial detachment of adjacent keratinocytes. Interestingly, SEM revealed intercellular clefts in the HaCaT cell monolayer immediately following the LICAP treatment. Plasma is highly oxidative[6,58]; therefore, the LICAP treatment could have triggered paracellular passage by oxidation of junctional proteins that are expressed and being attached together enclosing the paracellular route. The findings suggest that the activation of LICAP-induced TED may begin immediate after the treatment exposure, even before the time lag between mRNA and protein expression.

The results of the intracellular delivery assay with 3000–5000 Da FITC-dextran suggest that even cell-preserving exposure of LICAP treatment can facilitate the transcellular passage of large hydrophilic molecules through keratinocytes. Since the first report of plasma-assisted drug delivery into eukaryotic cells in 2005[29,30], there has been a steady stream of evidence for the potential of plasma in enhancing drug delivery, including the delivery of large, hydrophilic molecules[31,33–35,39,41,42,50,51] and genetic materials[29,30,32,33,36–38,46,48,63,64]. CAP treatment increases cell membrane permeability primarily through lipid peroxidation[43,45,47], which is thought to be linked to a number of processes such as intracellular calcium influx[65] and clathrin-dependent cell-membrane reuptake[49]. To the best of our knowledge, this is the first report of intracellular drug delivery by a plasma jet in human keratinocytes.

In clinical aspect, the immediacy and temporality of the LICAP-induced TED demonstrated in this study may be practical to clinicians considering the common practice process in dermatology clinics. Patients who undergo one or multiple types of energy-based device procedures, including plasma treatments, usually receive post-procedure skincare regimens. These regimens typically involve applying ointments, creams, or mask sheets containing beneficial substances to soothe the skin and enhance the effects of the procedure. The immediate and temporary increase in epidermal permeability induced by plasma treatment may improve the effectiveness of these skincare products, thereby enhancing the overall outcome of dermatological procedures.

Clinically, an additional consideration can be the sequence of plasma and topical agent application. Considering that the applied substance might be altered by the plasma, it seems prudent to apply plasma first and then the medicine for initial human applications. However, given the nascent state of this field, it is conceivable that future clinical or laboratory experiences might reveal specific substances that benefit from being applied before plasma treatment.

Another important aspect is the diverse physicochemical characteristics of medications, which must be considered in clinical practice. Our recent study in 2022 demonstrated significant whitening effects of LICAP on UV-induced hyperpigmentation additive effects with concurrent topical ascorbic acid in mouse skin[16]. It may suggest an example of a potent synergetic effect since ascorbic acid may broaden the therapeutic window by buffering excessive oxidative stress from LICAP and LICAP enhances the penetration of ascorbic acid. Our following study in 2023 showed that LICAP improved UV-induced wrinkles in mouse skin, with enhanced effects when used with poly-D, L-lactic acid nanoemulsion, a dermal fibroblast stimulator[17]. Combining these with the data from this study, it seems that practitioners with a sufficient understanding of the LICAP treatment technique and topical agents for concurrent therapy may select appropriate substances based on their therapeutic interests.

One of the potential limitations of this study is that the safety range of LICAP treatment was only evaluated in vitro. As a result, more research should be conducted to determine the clinical efficacy and safety of this treatment. Furthermore, the subjects for the expression level assay were limited to tight and adherens junctions. Perhaps the still-attached intercellular contacts in the SEM image were the focally distributed other classes of cell adhesion molecules, such as gap junctions and desmosomes. Finally, the safety range estimated in this study is only valid for the parameters we used (35.2 W power and 0.12 L/min helium gas). Further cytotoxicity data should be collected under various device parameter settings for the safe application of LICAP devices in a clinical setting.

In conclusion, this study estimated the minimal cytotoxicity range of LICAP exposure time and demonstrated that LICAP treatment can improve transepidermal penetration of the large hydrophilic molecule hEGF even within the estimated safety range. LICAP treatment appears to facilitate passage via both paracellular and transcellular routes. Future research is expected to include an assessment of the safety range of LICAP treatment in extended contexts as well as its clinical efficacy.

Data availability

The datasets used and/or analysed during the current study available from the corresponding author on reasonable request.

Received: 31 January 2024; Accepted: 12 December 2024
Published online: 16 January 2025

References

1. Lee, I. A. & Maibach, H. I. Pharmionics in dermatology. *Am. J. Clin. Dermatol.* **7**, 231–236 (2006).
2. Nestor, M. S. Combination therapy in clinical and cosmetic dermatology: the marriage of device and drug. *J. Drugs Dermatol.* **3**, S4–S11 (2004).

3. Ali, F. R. & Al-Niaimi, F. Laser-assisted drug delivery in dermatology: from animal models to clinical practice. *Lasers Med. Sci.* **31**, 373–381 (2016).
4. Mishra, D. K., Pandey, V., Maheshwari, R., Ghode, P. & Tekade, R. K. Cutaneous and transdermal drug delivery: techniques and delivery systems. *Basic Fundam. Drug Deliv.*. https://doi.org/10.1016/B978-0-12-817909-3.00015-7 (2018).
5. Akhtar, N., Singh, V., Yusuf, M. & Khan, R. A. Non-invasive drug delivery technology: Development and current status of transdermal drug delivery devices, techniques and biomedical applications. *Biomed. Tech.* **65**, 243–272 (2020).
6. Metelmann, H. R., von Woedtke, T. & Weltmann, K. D. *Comprehensive Clinical Plasma Medicine: Cold Physical Plasma for Medical Application. Comprehensive Clinical Plasma Medicine: Cold Physical Plasma for Medical Application* (Springer International Publishing, 2018). https://doi.org/10.1007/978-3-319-67627-2
7. Holcomb, J. D., Kelly, M., Hamilton, T. K. & DeLozier, J. B. A prospective study evaluating the use of helium plasma for dermal resurfacing. *Lasers Surg. Med.* **52**, 940–951 (2020).
8. Holcomb, J. D., Doolabh, V., Lin, M. & Zimmerman, E. High energy, double pass helium plasma dermal resurfacing: A prospective, multicenter, single-arm clinical study. *Lasers Surg. Med.* https://doi.org/10.1002/lsm.23524 (2022).
9. Lademann, O. et al. Drug delivery through the skin barrier enhanced by treatment with tissue-tolerable plasma. *Exp. Dermatol.* **20**, 488–490 (2011).
10. Kalghatgi, S., Tsai, C., Gray, R. & Pappas, D. Transdermal drug delivery using cold plasmas. *Ispc* 1–4 (2015).
11. Kristof, J., Miyamoto, H., Tran, A. N., Blajan, M. & Shimizu, K. Feasibility of transdermal delivery of Cyclosporine A using plasma discharges. *Biointerphases* **12**, 02B402 (2017).
12. Gelker, M., Müller-Goymann, C. C. & Viöl, W. Permeabilization of human stratum corneum and full-thickness skin samples by a direct dielectric barrier discharge. *Clin. Plasma Med.* **9**, 34–40 (2018).
13. Xin, Y., Wen, X., Hamblin, M. R. & Jiang, X. Transdermal delivery of topical lidocaine in a mouse model is enhanced by treatment with cold atmospheric plasma. *J. Cosmet. Dermatol.* **20**, 626–635 (2021).
14. Xin, Y., Wen, X. & Jiang, X. Analgesic effect of topical lidocaine is enhanced by cold atmospheric plasma pretreatment in facial CO2 laser treatments. *J. Cosmet. Dermatol.* **20**, 2794–2799 (2021).
15. Nam, S. H. et al. Improved penetration of wild ginseng extracts into the skin using low-temperature atmospheric pressure plasma. *Plasma Sources Sci. Technol.* **27** (2018).
16. Ahn, G. R. et al. Low-intensity cold atmospheric plasma reduces wrinkles on photoaged skin through hormetic induction of extracellular matrix protein expression in dermal fibroblasts. *Lasers Surg. Med.* **54**, 978–993 (2022).
17. Ahn, G. R. et al. The effect of low-intensity cold atmospheric plasma jet on photoaging-induced hyperpigmentation in mouse model. *J. Cosmet. Dermatol.* 1–11. https://doi.org/10.1111/jocd.15778 (2023).
18. Lee, H. Y., Choi, J. H., Hong, J. W., Kim, G. C. & Lee, H. J. Comparative study of the Ar and He atmospheric pressure plasmas on E-cadherin protein regulation for plasma-mediated transdermal drug delivery. *J. Phys. D Appl. Phys.* **51**, 215401 (2018).
19. Choi, J. H. et al. Treatment with low-temperature atmospheric pressure plasma enhances cutaneous delivery of epidermal growth factor by regulating E-cadherin-mediated cell junctions. *Arch. Dermatol. Res.* **306**, 635–643 (2014).
20. Zhang, Y. et al. Advances in transdermal insulin delivery. *Adv. Drug Deliv. Rev.* **139**, 51–70 (2019).
21. Ita, K. Transdermal delivery of vaccines—Recent progress and critical issues. *Biomed. Pharmacother.* **83**, 1080–1088 (2016).
22. Prausnitz, M. R. & Langer, R. Transdermal drug delivery. *Nat. Biotechnol.* **26**, 1261–1268 (2008).
23. Wen, X., Xin, Y., Hamblin, M. R. & Jiang, X. Applications of cold atmospheric plasma for transdermal drug delivery: a review. *Drug Deliv. Transl. Res.* https://doi.org/10.1007/s13346-020-00808-2 (2020).
24. Brunner, J., Ragupathy, S. & Borchard, G. Target specific tight junction modulators. *Adv. Drug Deliv. Rev.* **171**, 266–288 (2021).
25. Stoffels, E., Kieft, I. E. & Sladek, R. E. J. Superficial treatment of mammalian cells using plasma needle. *J. Phys. D Appl. Phys.* **36**, 2908 (2003).
26. Kieft, I. E. et al. Electric discharge plasmas influence attachment of cultured CHO K1 cells. *Bioelectromagnetics* **25**, 362–368 (2004).
27. Blackert, S., Haertel, B., Wende, K., von Woedtke, T. & Lindequist, U. Influence of non-thermal atmospheric pressure plasma on cellular structures and processes in human keratinocytes (HaCaT). *J. Dermatol. Sci.* **70**, 173–181 (2013).
28. Hoentsch, M. et al. Persistent effectivity of gas plasma-treated, long time-stored liquid on epithelial cell adhesion capacity and membrane morphology. *PLoS One*. **9**, e104559 (2014).
29. Ogawa, Y. et al. An epoch-making application of discharge plasma phenomenon to gene-transfer. *Biotechnol. Bioeng.* **92**, 865–870 (2005).
30. Sakai, Y. et al. A novel transfection method for mammalian cells using gas plasma. *J. Biotechnol.* **121**, 299–308 (2006).
31. Ramachandran, N., Jaroszeski, M. & Hoff, A. M. Molecular delivery to cells facilitated by corona ion deposition. *IEEE Trans. Nanobiosci.* **7**, 233–239 (2008).
32. Leduc, M., Guay, D., Leask, R. L. & Coulombe, S. Cell permeabilization using a non-thermal plasma. *New. J. Phys.* **11** (2009).
33. Connolly, R. J., Lopez, G. A., Hoff, A. M. & Jaroszeski, M. J. Characterization of plasma mediated molecular delivery to cells in vitro. *Int. J. Pharm.* **389**, 53–57 (2010).
34. Sasaki, S., Kanzaki, M. & Kaneko, T. Highly efficient and minimally invasive transfection using time-controlled irradiation of atmospheric-pressure plasma. *Appl. Phys. Express* **7** (2014).
35. Kaneko, T. et al. Improvement of cell membrane permeability using a cell-solution electrode for generating atmospheric-pressure plasma. *Biointerphases* **10**, 029521 (2015).
36. Ikeda, Y., Motomura, H., Kido, Y., Satoh, S. & Jinno, M. Effects of molecular size and chemical factor on plasma gene transfection. *Jpn. J. Appl. Phys.* **55** (2016).
37. Jinno, M., Ikeda, Y., Motomura, H., Kido, Y. & Satoh, S. Investigation of plasma induced electrical and chemical factors and their contribution processes to plasma gene transfection. *Arch. Biochem. Biophys.* **605**, 59–66 (2016).
38. Xu, D. et al. Intracellular ROS mediates gas plasma-facilitated cellular transfection in 2D and 3D cultures. *Sci. Rep.* **6**, 1–14 (2016).
39. Sasaki, S. et al. Roles of charged particles and reactive species on cell membrane permeabilization induced by atmospheric-pressure plasma irradiation. *Jpn. J. Appl. Phys.* **55** (2016).
40. Jinno, M., Tachibana, K., Motomura, H., Saeki, N. & Satoh, S. Improvement of efficiency and viability in plasma gene transfection by plasma minimization and optimization electrode configuration. *Jpn. J. Appl. Phys.* **55** (2016).
41. Sasaki, S. et al. Characterization of plasma-induced cell membrane permeabilization: Focus on OH radical distribution. *J. Phys. D Appl. Phys.* **49**, 334002 (2016).
42. Vijayarangan, V. et al. Cold atmospheric plasma parameters investigation for efficient drug delivery in HeLa cells. *IEEE Trans. Radiat. Plasma Med. Sci.* **2**, 109–115 (2017).
43. Van Der Paal, J., Verheyen, C., Neyts, E. C. & Bogaerts, A. Hampering effect of cholesterol on the permeation of reactive oxygen species through phospholipids bilayer: possible explanation for plasma cancer selectivity. *Sci. Rep.* **7**, 1–11 (2017).
44. Kaneko, T., Sasaki, S., Takashima, K. & Kanzaki, M. Gas-liquid interfacial plasmas producing reactive species for cell membrane permeabilization. *J. Clin. Biochem. Nutr.* **60**, 3–11 (2017).
45. Yusupov, M., Van der Paal, J., Neyts, E. C. & Bogaerts, A. Synergistic effect of electric field and lipid oxidation on the permeability of cell membranes. *Biochim. Biophys. Acta Gen. Subj.* **1861**, 839–847 (2017).
46. Jinno, M. et al. Synergistic effect of electrical and chemical factors on endocytosis in micro-discharge plasma gene transfection. *Plasma Sources Sci. Technol.* **26** (2017).
47. Van der Paal, J., Fridman, G. & Bogaerts, A. Ceramide cross-linking leads to pore formation: Potential mechanism behind CAP enhancement of transdermal drug delivery. *Plasma Process. Polym.* **16**, 1–10 (2019).

48. Hiramatsu, T., Hirashige, H., Kido, Y., Satoh, S. & Jinno, M. Importance of collision frequency in the molecular size dependency of gene transfer efficiency in the surface discharge method. *Jpn. J. Appl. Phys.* **58** (2019).
49. He, Z. et al. Cold atmospheric plasma stimulates clathrin-dependent endocytosis to repair oxidised membrane and enhance uptake of nanomaterial in glioblastoma multiforme cells. *Sci. Rep.* **10**, 1–12 (2020).
50. Haralambiev, L. et al. The effect of cold atmospheric plasma on the membrane permeability of human osteosarcoma cells. *Anticancer Res.* **40**, 841–846 (2020).
51. Haralambiev, L. et al. Cold atmospheric plasma treatment of chondrosarcoma cells affects proliferation and cell membrane permeability. *Int. J. Mol. Sci.* **21** (2020).
52. van Meerloo, J., Kaspers, G. J. L. & Cloos, J. Cell sensitivity assays: the MTT assay. *Cancer Cell Cult.*, 237–245. https://doi.org/10.1007/978-1-61779-080-5_20 (2011).
53. Biological Evaluation of Medical Devices. *Part 5: Tests for in Vitro Cytotoxicity*, Vol. 40 (International Organization for Standardization, 2009).
54. Ross, E. V., Grossman, M. C., Duke, D. & Grevelink, J. M. Long-term results after CO2 laser skin resurfacing: a comparison of scanned and pulsed systems. *J. Am. Acad. Dermatol.* **37**, 709–718 (1997).
55. Ross, E. V., McKinlay, J. R. & Anderson, R. R. Why does carbon dioxide resurfacing work? A review. *Arch. Dermatol.* **135**, 444–454 (1999).
56. Hwang, S. G., Kim, J. H., Jo, S. Y., Kim, Y. J. & Won, C. H. Cold atmospheric plasma prevents wrinkle formation via an antiaging process. *Plasma Med.* **10**, 91–102 (2020).
57. Nikiforov, A. Y., Leys, C., Gonzalez, M. A. & Walsh, J. L. Electron density measurement in atmospheric pressure plasma jets: Stark broadening of hydrogenated and non-hydrogenated lines. *Plasma Sources Sci. Technol.* **24** (2015).
58. Von Woedtke, T., Emmert, S., Metelmann, H. R., Rupf, S. & Weltmann, K. D. Perspectives on cold atmospheric plasma (CAP) applications in medicine. *Phys. Plasmas* **27** (2020).
59. Van Der Paal, J., Aernouts, S., Van Duin, A. C. T., Neyts, E. C. & Bogaerts, A. Interaction of O and OH radicals with a simple model system for lipids in the skin barrier: A reactive molecular dynamics investigation for plasma medicine. *J. Phys. D Appl. Phys.* **46** (2013).
60. Marschewski, M. et al. Electron spectroscopic analysis of the human lipid skin barrier: Cold atmospheric plasma-induced changes in lipid composition. *Exp. Dermatol.* **21**, 921–925 (2012).
61. Marwah, H., Garg, T., Goyal, A. K. & Rath, G. Permeation enhancer strategies in transdermal drug delivery. *Drug Deliv.* **23**, 564–578 (2016).
62. Hu, Y. J., Wang, Y. D., Tan, F. Q. & Yang, W. X. Regulation of paracellular permeability: Factors and mechanisms. *Mol. Biol. Rep.* **40**, 6123–6142 (2013).
63. Chalberg, T. W. et al. Gene transfer to rabbit retina with electron avalanche transfection. *Investig. Ophthalmol. Vis. Sci.* **47**, 4083–4090 (2006).
64. Edelblute, C. M., Heller, L. C., Malik, M. A. & Heller, R. Activated air produced by shielded sliding discharge plasma mediates plasmid DNA delivery to mammalian cells. *Biotechnol. Bioeng.* **112**, 2583–2590 (2015).
65. Sasaki, S., Kanzaki, M. & Kaneko, T. Calcium influx through TRP channels induced by short-lived reactive species in plasma-irradiated solution. *Sci. Rep.* **6**, 1–11 (2016).

Acknowledgements

This work was supported by the Institute of Information & Communications Technology Planning & Evaluation (IITP) grant funded by the Korean government (MSIT) (No. 2021-0-01074, Development of Intelligent Plasma Medical Device Applying User Data Platform Technology Project) and Chung-Ang University Research Grants in 2024. One of the authors, Ga Ram Ahn, is a shareholder of the cooperation that provided the test device. All other authors declare no conflicts of interest.

Author contributions

Conceptualization: BJ Kim, KB Lee, J Seok. Data curation: HS Han, WG Lee, KH Yoo. Formal analysis: YJ Kim. Investigation: MG Song, HS Han. Methodology: WG Lee, KH Yoo. Project administration: J Seok. Software: MG Song, WG Lee. Validation: KH Yoo. Visualization: KB Lee, BJ Kim. Writing—original draft: GR Ahn, HJ Park. Writing—review and editing: all authors.

Declarations

Competing interests

This work was supported by the Institute of Information and Communications Technology Planning and Evaluation (IITP) grant funded by the Korean government (MSIT) (No. 2021-0-01074, Development of Intelligent Plasma Medical Device Applying User Data Platform Technology Project) and Chung-Ang University Research Grants in 2024. One of the authors, Ga Ram Ahn, is a shareholder of the cooperation that provided the test device. All other authors declare no conflicts of interest.

Additional information

Supplementary Information The online version contains supplementary material available at https://doi.org/10.1038/s41598-024-83201-0.

Correspondence and requests for materials should be addressed to J.S., K.B.L. or B.J.K.